Nuclear Inst. and Methods in Physics Research, A 924 (2019) 153–159

Contents lists available at ScienceDirect

Nuclear Inst. and Methods in Physics Research, A

journal homepage: www.elsevier.com/locate/nima

Measurement of the charge collection in irradiated miniature sensors for the upgrade of the ATLAS phase-II strip tracker

V. Cindro [d,*], S.H. Abidi [i], A.A. Affolder [h], M. Arratia [a], B. Ciungu [i], K. Dette [i], Z. Dolezal [g], C. Escobar [c], V. Fadeyev [h], C. García [c], I.M. Gregor [b], K. Hara [j], L.B.A. Hommels [a], Y. Ikegai [e], P. Kodys [g], G. Kramberger [d], J. Kroll [k], C. Lacasta [c], V. Latonova [k], D. Madaffari [c], I. Mandić [d], M. Mikestikova [k], M. Mikuž [d,f], M. Miñano [c], K. Nakamura [e], R.S. Orr [i], D. Rodriguez [c], E. Rossi [b], C. Solaz [c], U. Soldevila [c], J. Suzuki [j], R. Teuscher [i], Y. Unno [e], S. Wada [j]

[a] Cavendish Laboratory, University of Cambridge, JJ Thomson Avenue, Cambridge CB3 0HE, United Kingdom
[b] Deutsches Elektronen-Synchrotron, Notkestraße 85, 22607 Hamburg, Germany
[c] Instituto de Física Corpuscular (IFIC) - CSIC-University of Valencia, Parque Científico, C/Catedrático José Beltrán 2, E-46980 Paterna, Spain
[d] Experimental Particle Physics Department, Jožef Stefan Institute, Jamova 39, SI-1000 Ljubljana, Slovenia
[e] IPNS, KEK, 1-1 Oho, Tsukuba, Ibaraki 305-0801, Japan
[f] Faculty of Mathematics and Physics, University of Ljubljana, Jadranska ulica 19, SI-1000 Ljubljana, Slovenia
[g] Faculty of Mathematics and Physics, Charles University, V Holesovickach 2, Prague, CZ18000, Czech Republic
[h] Santa Cruz Institute for Particle Physics (SCIPP), University of California, Santa Cruz, CA 95064, USA
[i] Department of Physics, University of Toronto, 60 Saint George St., Toronto M5S 1A7, Ontario Canada
[j] Institue of Pure and Applied Sciences, University of Tsukuba, 1-1-1 Tennodai, Tsukuba, Ibaraki 305-8571, Japan
[k] Academy of Sciences of the Czech Republic, Institute of Physics, Na Slovance 2, 18221, Prague 8, Czech Republic

ARTICLE INFO

Keywords:
Silicon
Microstrip
Signal
ATLAS
Upgrade
Radiation

ABSTRACT

Miniature sensors with external dimensions of 10 mm x 10 mm were produced together with full-size sensors for the innermost ring (R0) of the end-cap part in the upgraded ATLAS inner tracker (ITk). AC- and DC-coupled n-type strips with three different pitches (wide, default and narrow) were processed on high-resistivity p-type FZ silicon substrates by Hamamatsu Photonics. The miniature sensors were irradiated with 70-MeV protons at CYRIC, Tohoku University (Japan) and reactor neutrons at the Jožef Stefan Institute (Slovenia) to three different 1-MeV neutron equivalent fluences: 0.5, 1 and 2 x 10^{15} $n_{eq}cm^{-2}$. The upper fluence range exceeds the highest anticipated in the innermost part of the ATLAS ITk-Strips over the HL-LHC lifetime (~1.25 × $10^{15}n_{eq}cm^{2}$). The charge collection in the test sensors was evaluated systematically using a ^{90}Sr β-source and an Alibava analogue readout system at reverse-bias voltages up to 1000 V.

Contents

* Correspondence to: Jožef Stefan Institute, Jamova 39, 100 Ljubljana, Slovenia.
E-mail address: vladimir.cindro@ijs.si (V. Cindro).

https://doi.org/10.1016/j.nima.2018.10.007
Received 9 March 2018; Received in revised form 27 September 2018; Accepted 2 October 2018
Available online 15 October 2018

1. Introduction

The Large Hadron Collider (LHC) will be upgraded to operate at higher luminosities (HL-LHC), with its peak luminosity expected to be about L = 7.5 10^{34} $cm^{-2}s^{-1}$, having approximately 200 collisions per bunch crossing. As the existing tracking systems of the ATLAS detector cannot cope with this high multiplicity, the ATLAS collaboration [1] will completely upgrade its inner detector during Phase II (2024–26) [2]. The inner detector, which provides the track information about the crossing particles, will be replaced by an all-silicon tracking system with strip sensors in the outer part and pixel sensors in the inner part. The strip-detector part will consist of 4 barrel layers and 6 disks in each end-cap (EC) region. A sensor type of an n-strip on a p-bulk geometry [3] was chosen as the best solution since p-bulk does not invert with radiation and the np junction remains on the same side, which allows a partially depleted operation. The collection of electrons on the readout-strip electrodes has a further advantage compared to sensors with p electrodes, since the electrons drift faster and have longer trapping distances with respect to the holes. Prototype sensors were already produced and extensively studied [4,5]. The subject of this paper is the measurements made on sensors produced in the prototype batch for the end-cap region of the ATLAS detector.

2. Samples

The samples were miniature n-in-p strip sensors (ATLAS12EC-R0 or shortly R0 sensors) delivered at the beginning of 2017 and produced by Hamamatsu on the same p-type 6-inch wafers as the full-size annular sensors for the first ring (R0) of the ATLAS ITk end-cap strip detector [6]. The strip pitch of the full size end-cap sensors ranges from 70 μm to 84 μm; therefore, miniature sensors with three different pitches (70 μm, narrow; 75.5 μm, default; and 84 μm, wide) were produced to determine how the properties of the sensors vary with the pitch of the strips. The outer dimensions of the miniature sensors are 10 mm ×10 mm, with each sensor having 104 8 mm-long readout strips. The strips are biased through 1.5 MΩ polysilicon resistors. The readout electronics is AC coupled to the n-type implant via aluminum metallization extending over the implant. Regular measurements of the charge collection will also be performed on a small number of these sensors during the production for the ATLAS upgrade as a part of a Q&A procedure. More details about the design of the sensor are presented in [7].

3. Irradiations

The sensors in ATLAS will be exposed to high fluences of charged particles and neutrons [2]. The non-ionizing energy loss (NIEL) of the charged particles will be dominant at the smaller radii, while the contribution of neutrons becomes more important in the outer region, where the strip detectors will be placed. To evaluate the damage and degradation of the detectors' performance, irradiations of the sensors with charged particles and neutrons and measurements of their properties are required. Therefore, we performed irradiations with 70 MeV protons at CYRIC (Cyclotron and Radioisotope Center, Tohoku University, Japan) and with neutrons at the TRIGA reactor (Jožef Stefan Institute, Ljubljana, Slovenia).

The maximum 1 MeV neutron equivalent fluences for the barrel and strip end-cap detectors are predicted to be 2.8 10^{14} $n_{eq}cm^{-2}$ and 8.2 10^{14} $n_{eq}cm^{-2}$, respectively [2]. In addition, a safety factor of 1.5 is required to exclude the effects of possible uncertainities in the simulation. We irradiated the miniature sensors to three different equivalent fluences: 0.5 10^{15} $n_{eq}cm^{-2}$, 1 10^{15} $n_{eq}cm^{-2}$ and 2 10^{15} $n_{eq}cm^{-2}$. The highest fluence allows an interpolation of the measured values, even for fluences higher than we expect in ATLAS. All irradiations were performed without bias on the sensors.

At CYRIC the holder with the samples was moved through the proton beam to allow for uniform irradiation. Cold gas from liquid nitrogen was then flushed around the samples to maintain a temperature of approximately −15 °C. The dosimetry of the protons was made with aluminum foils attached to the samples, with the fluence uncertainty being approximately 10%. A more detailed description of the irradiations with protons and scaling to equivalent fluences can be found in [4]. After the irradiation the samples were stored in a freezer to prevent annealing before mounting in the experimental setup.

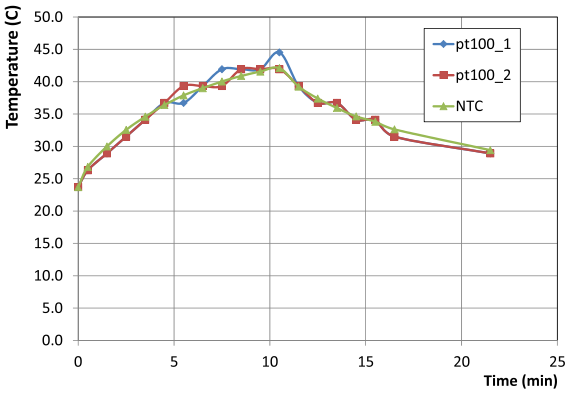

Fig. 1. Temperature of silicon sensor measured with three different sensors during irradiation at the full reactor power (250 kW). After 10 min sensor was pulled out of the reactor core.

The irradiations with neutrons were performed by the insertion of small polyethylene telephthalate (PET) containers with samples into the reactor core. The samples were irradiated at the full reactor power (250 kW) with a uniform flux of neutrons (Φ_{eq} = 1.54 10^{12} $n_{eq}cm^{-2}s^{-1}$). The fluence was determined with the irradiation time being in the range from 330 s to 1320 s. The samples were not biased and were not cooled during the irradiation; however, they were put into the fridge as soon as the activation dropped to an acceptable level (approx. ten minutes after the irradiation). The temperature of the water in the reactor tank is about 20 °C, while the temperature of the sample reaches about 40 °C during the irradiation (Fig. 1.). Taking into account the activation energy for short-term annealing (1.1 eV [8]) we can estimate that annealing at 40 °C is about 20 times faster than at 20 °C. Therefore, the annealing during the irradiation is at a comparable level to annealing during the assembly of sensors as part of the setup, which took about 1–2 h at room temperature. It is negligible compared to the 80 min annealing on 60 °C temperature.

The spectrum of reactor neutrons is continuous in the energy range from thermal to several MeV [9]. The 1 MeV neutron-equivalent nonionizing loss fluences were determined with the measurements of leakage currents in the silicon diodes [10] and verified with calculations [11]. The fluence uncertainty is approximately 10%.

4. I/V and C/V measurements

The leakage current as a function of bias voltage was measured for the non-irradiated and proton-irradiated samples (Fig. 2), with all three different pitches (default, narrow and wide). It was measured with a delay of 10 s after setting the reverse-bias voltage. For the non-irradiated sensors the IV characteristics were measured at 20 °C up to 600 V, while for the irradiated sensors it was measured at −30 °C and up to 1000 V. Before the measurements the samples were annealed for 80 min at 60 °C. There were no observed onsets of micro-discharges with respect to any of them. For all the tested detectors the leakage current before irradiation was less than 4 $nAcm^{-2}$, well below the technical specification limit (100 $nAcm^{-2}$). The smooth behavior of the leakage current was also measured after the irradiation and no systematic dependence on the strip pitch was observed.

The measured values of the leakage current per cm^2 at 700 V and after 80 min of annealing are compared with the measurements

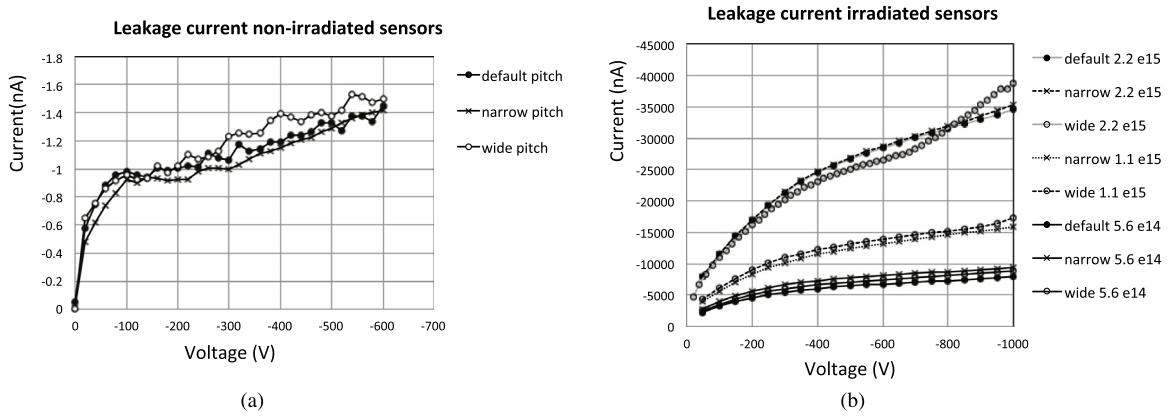

Fig. 2. Leakage current measured for proton irradiated sensors with default (75.5 μm), narrow (70 μm) and wide (84 μm) pitches as a function of the bias voltage. The current was measured at 20 °C for the non-irradiated (a) and at −30 °C for the irradiated sensors (b). The values for the irradiated sensors are measured after annealing, and they are normalized to −20 °C according to the scaling given in [12]. All fluences are in the units of $n_{eq}cm^{-2}$.

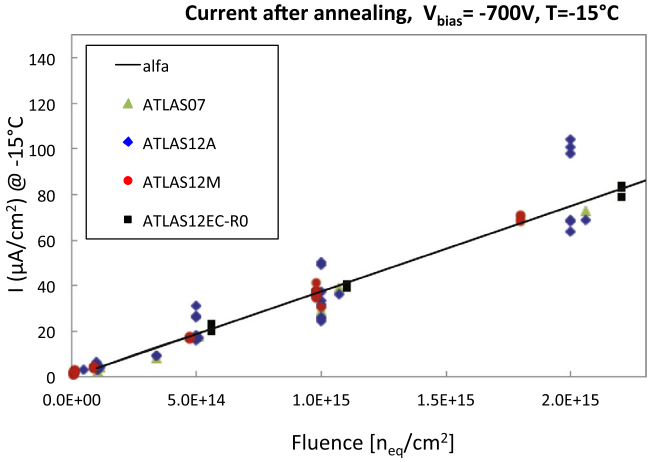

Fig. 3. Leakage current measured on ATLAS12EC-R0 miniature sensors at 700 V bias voltage and normalized to −15 °C. Straight line represents the values calculated from the leakage current constant $\alpha = 4.0\ 10^{-17}$ A/cm normalized to −15 °C. The measurements on sensors ATLAS07, ATLAS12A and ATLAS12M miniature sensors are from [13].

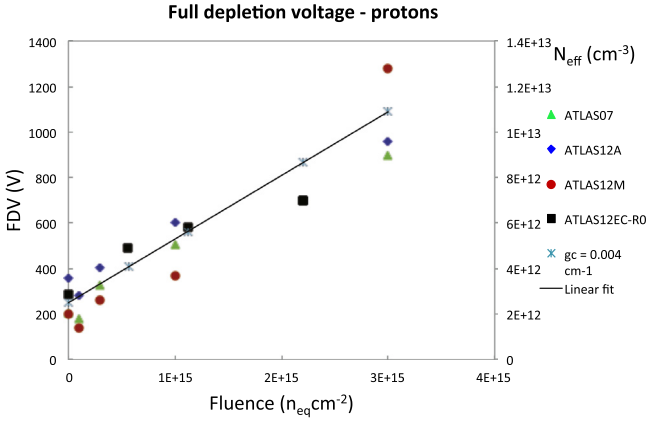

Fig. 4. Full depletion voltages measured in different batches of the ATLAS prototypes. Measurements of the ATLAS12EC-R0 sensors are described in this paper, while the measurements for the other sensors are from [13]. The drop in the full depletion voltage after irradiation to 10^{14} $n_{eq}cm^{-2}$ indicates acceptor removal in the p-type bulk.

on the miniature sensors produced during previous sensor-production runs [13] (Fig. 3). The values are normalized to −15 °C with scaling $I \alpha T^2 e^{-1.21\ eV/kT}$ [12]. They all agree well with the value obtained from a leakage current constant $\alpha = 4.0\ 10^{-17}$ A/cm [10]. Agreement is good, even at the highest fluence, indicating that at a bias of 700 V the whole detector volume contributes to the leakage current.

The full depletion voltage of the annealed sensors was determined from the fit of the straight lines to the measured $1/C^2$ plot. The C-V measurements were performed at −10 °C and at 1 kHz. It is known that the measured values for irradiated detectors depend on the frequency and temperature [14], and that the electric field in highly irradiated silicon detectors is not linear, as would be expected in a simple model [15]. However, this value was chosen to be compatible with the measurements of previous batches. The results are summarized in Fig. 4. The full depletion voltages calculated with a stable acceptor creation rate g_c are also shown as a comparison. There is no clear evidence for the removal of the initial acceptors in the ATLAS12EC-R0 sensors. The initial acceptor removal can be observed at the low fluence (10^{14} $n_{eq}cm^{-2}$) in previous measurements, which are also shown in this plot. There are no measurements at low fluences for the ATLAS12EC-R0 sensors to show this effect that can be seen as a drop in the full depletion voltage measured after an irradiation to 10^{14} $n_{eq}cm^{-2}$.

The increase of the effective dopant concentration after the neutron irradiation was too high to be measured with the C-V method since voltages well above 1000 V should be applied, even at the lowest fluence (5 10^{14} $n_{eq}cm^{-2}$) to obtain reasonable curves from which the full depletion voltage could be estimated.

5. Measurements of the charge collection

5.1. Experimental setup

The signals generated in the silicon sensors with the ^{90}Sr source were recorded with the Alibava readout system [16]. The signals are amplified in the analogue frontend electronics with a 25 ns peaking time. The amplifiers are integrated into a Beetle readout chip [17]. The Alibava system samples the analogue signals with a 40 MHz clock frequency, while the scintillator set underneath the sample triggers the readout cycle. Only the signals sampled in a certain time window (10 ns) of the delay measured relative to the clock signal are used in the analysis. The spread of the signal over the strips is taken into account with a clustering algorithm that has a seed threshold of 3.5 times the channel's average noise level and a neighbor threshold of 1.5 times the noise. A Landau function convoluted with a Gaussian was fitted to the distribution of the measured signals and the most probable signal obtained from the fit was defined as a measure of the collected charge. The measurements were performed with three setups (Ljubljana, KEK, Valencia), each using several boards with Beetle chips. Amplification of the Beetle input stage depends on the control parameters; therefore,

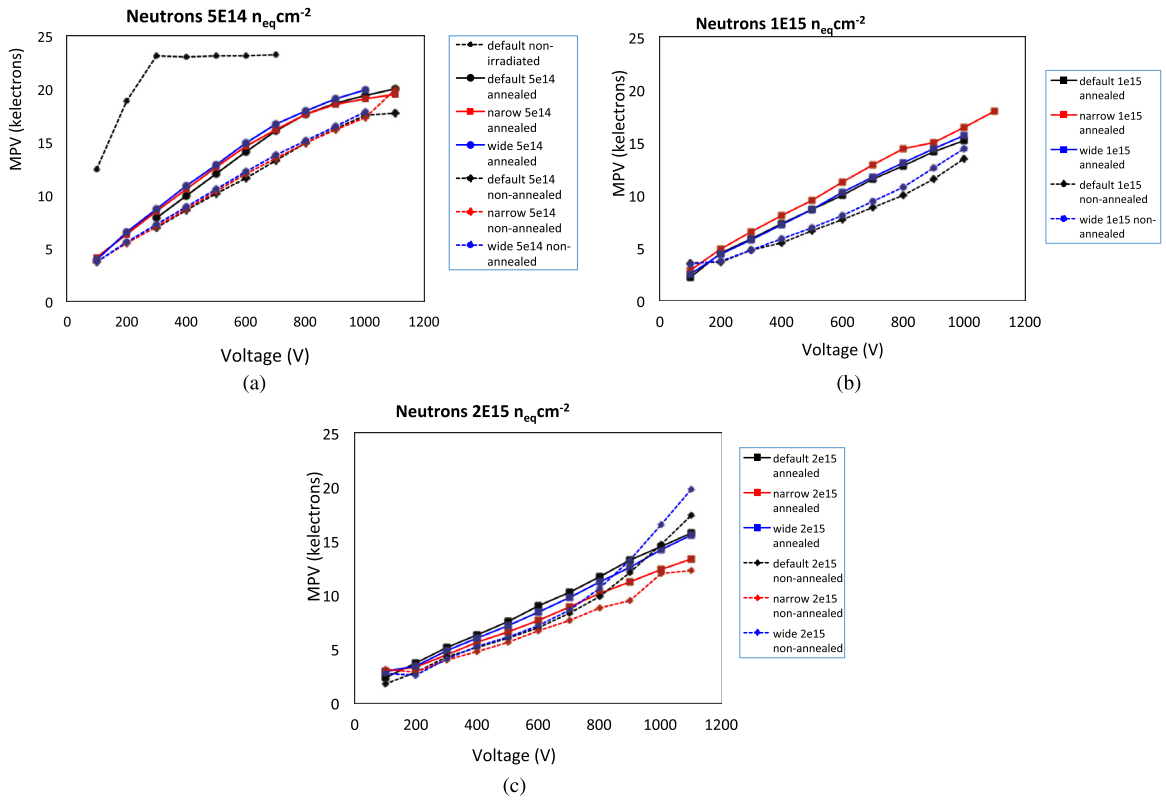

Fig. 5. Most probable value of the collected charge as a function of the bias voltage measured after the irradiation with neutrons to 5 10^{14} $n_{eq}cm^{-2}$ (a), 10^{15} $n_{eq}cm^{-2}$ (b) and 2 10^{15} $n_{eq}cm^{-2}$ (c). Dashed lines represent measured values before annealing, and solid lines after 80 min of annealing at 60 °C. As a comparison the values measured before the irradiation are shown (a).

the calibration procedure was applied to reduce the 10% board-to-board variations. Since the internal calibration is sensitive to the fine-tuning of the timing, we calibrated the setups and boards with measurements on non-irradiated samples. We assumed full charge collection above the full depletion voltage: 23100 e^- for a sensor with a 300 μm active depth [4]. All the sensors were measured at the same temperature, since amplification of the Beetle chip also depends on the temperature. The noise of the system was between 800 e and 900 e for all the measurements and is correlated with the leakage current of the sensor.

5.2. Dependence of the charge collection on the bias voltage

The results of the voltage scans of the charge measurements for neutron-irradiated sensors are shown in Fig. 5, before and after 80 min of annealing at 60 °C. This annealing time was chosen to minimize the effects of the annealing on the results: short-term annealing of the effective dopant concentration is completed and the effect of long-term annealing is still small [18]. Short-term annealing improves the collection of charge as a result of two effects: the effective dopant concentration drops [18] and the trapping time for the electrons becomes longer [19]. In the case of the irradiated n-in-p strip sensors the electrons make the dominant contribution to the signal, since they drift faster than the holes and move towards the region of the larger weighting field close to the n-strip. The temperature during the measurement was measured close to the silicon sensor at a cooling block connected to a Peltier cooler. The samples were cooled to −20 °C.

The collected charge increases with the applied voltage and even at the lowest fluence does not saturate at high voltages since larger electric fields increase the drift velocity and reduce the trapping. The results of the measurement with a non-irradiated detector are also shown in Fig. 5a. After reaching the bias voltage of approximately 300 V, the collected charge remains constant, in agreement with the measurement of the full depletion voltage with C-V measurements, which gave a value of 280–290 V. The strip width does not influence the size of the signal, except at the highest fluence and high voltages above approximately 800 V. This can be explained by the onset of the charge multiplication [20]. Before annealing the effective dopant concentration is high enough to cause large electric fields close to the strips at high voltages in which multiplication occurs. The weighting field is higher in the vicinity of wider strips, since the distance between the strips is smaller compared to the narrower strips. The effect of the multiplication which occurs close to the strips is more evident there, compared to the narrower strips.

The results measured with the proton-irradiated sensors are shown in Fig. 6, where the results for the sensors with the default pitch are presented before and after short-term annealing. As with the neutrons, the short-term annealing improves the charge collection since the effective dopant concentration drops.

For a comparison, the fluence dependence for the neutron- and proton-irradiated sensors is shown in Fig. 7 for two bias voltages: 500 V and 700 V. The charge collection of the proton-irradiated sensors is higher than that of the neutron-irradiated sensors. The reason for this is the lower introduction rate of stable effects with protons than for neutrons [21]. The applied voltages were not high enough to establish the electric field in the whole volume of the neutron-irradiated detectors, even at the lowest fluence. Therefore, the electric field in the neutron-irradiated detectors does not extend as deep as in the proton-irradiated detectors and there is less charge generated in the active volume. This effect was shown with edge TCT measurements [4]. The slightly higher trapping of the charge carriers after the proton irradiation did not reduce this difference.

The aim of this study was also to compare the measured charge collection with the measurement on the previous batch of ATLAS sensors (A12) [4]. The voltage dependence for the non-irradiated as well as the neutron-irradiated A12 and R0 sensors is summarized in Fig. 8. Before the irradiation the only difference is below the full depletion voltage, which was slightly higher for the A12 (350 V) compared to the R0

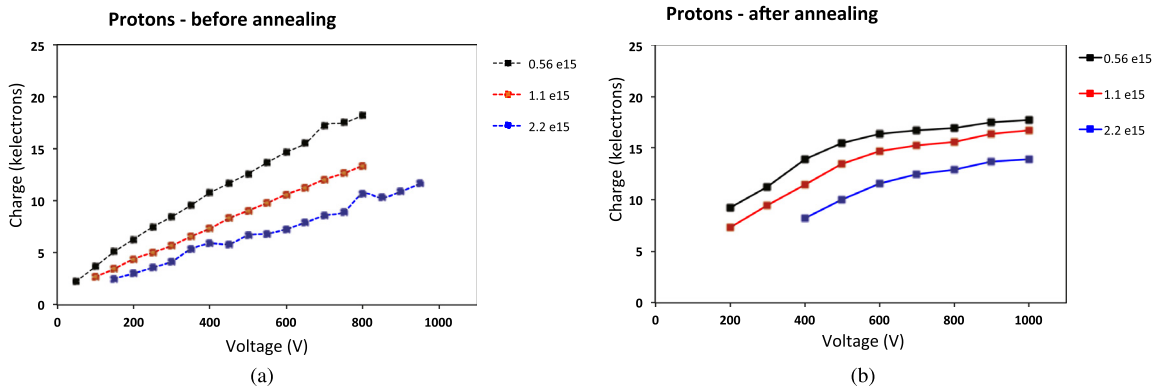

Fig. 6. Most probable value of the collected charge of the proton-irradiated sensors before (a) and after annealing (b).

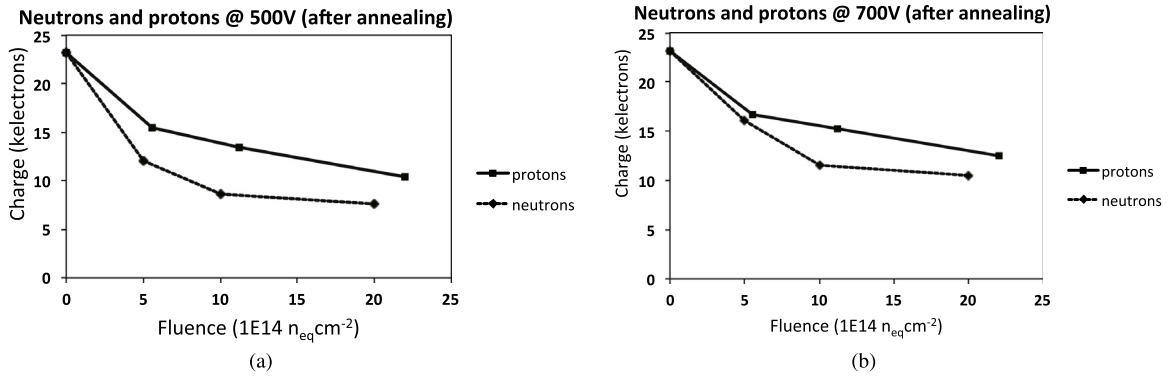

Fig. 7. Fluence dependence of the collected charge measured at 500 V (a) and 700 V (b).

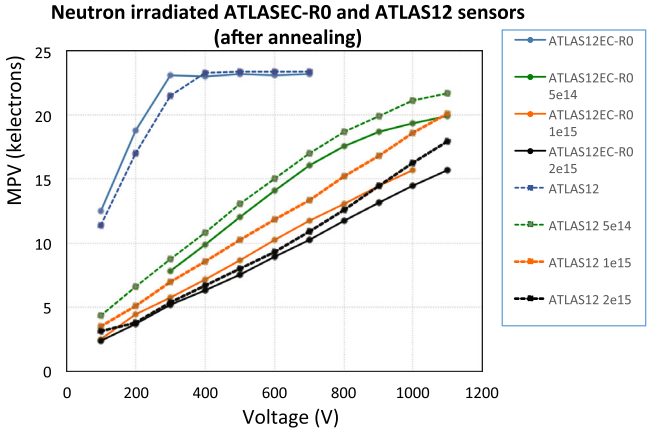

Fig. 8. Comparison of the measured charge in the ATLAS12EC-R0 and A12 sensors. Fluences are expressed in the units of $n_{eq}cm^{-2}$.

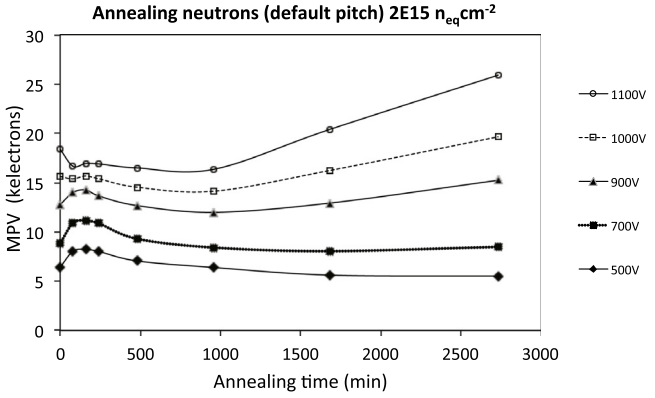

Fig. 9. Collected charge at different voltages measured after annealing at 60 °C. Measurements were taken at −20 °C. The sensor was irradiated with neutrons to 2 10^{15} $n_{eq}cm^{-2}$.

(290 V). The difference is due to the lower wafer resistivity at which the A12 sensors were produced (3.1 kΩ compared to 3.5 kΩ). Above full depletion both sensors give an approximately 23 ke⁻ signal, which means that they have the same active depth.

At the highest fluence expected in the ATLAS strip detector (~1.25 × $10^{15}n_{eq}cm^2$) the signal expected at 500 V after proton irradiation is about 13 ke⁻ and about 8 ke⁻ after neutron irradiation. At 700 V these numbers are 15 ke⁻ and 11 ke⁻. Assuming that the damages after the proton and neutron irradiations are additive [22], with a 50% mixture of protons and neutrons an approximately 10.5 ke⁻ signal is expected at 500 V and a 13 ke⁻ signal at 700 V. This is in agreement with the data obtained in the previous measurements [2,4].

5.3. Annealing of the charge collection

We performed long-term annealing at 60 °C on the ministrip sensor with a default pitch and irradiated with neutrons to 2 10^{15} $n_{eq}cm^{-2}$. The charge-collection measurements taken at −20 °C during annealing intervals for voltages between 500 V and 1100 V in 100 V steps are shown in Fig. 9. The longest annealing time was 164 h. At lower voltages and shorter annealing times the measured charge first increases with time and reaches its maximum after approximately 160 min, then it starts to decrease. This behavior is to be expected due to the change of the effective dopant concentration. The slight shift of the maximum in time (160 min) compared to the measurements of effective dopant concentration (80 min) can be explained by the effect of annealing on the electron-trapping time. It increases over several

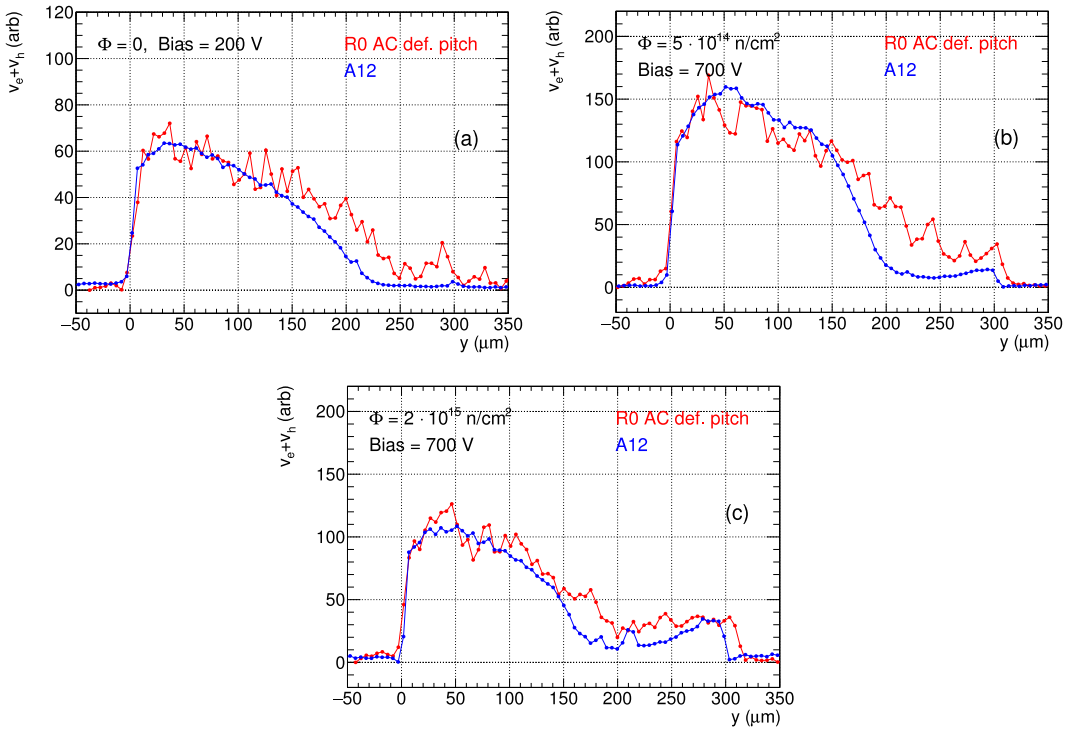

Fig. 10. Velocity profile measured with the edge TCT method in the ATLAS12EC-R0 and A12 sensors for non-irradiated sensors (a), after irradiation with neutrons to 5 10^{14} $n_{eq}cm^{-2}$ (b) and 2 10^{15} $n_{eq}cm^{-2}$ (c). The sum of electron and hole velocities is probed by the rise of the signal [23].

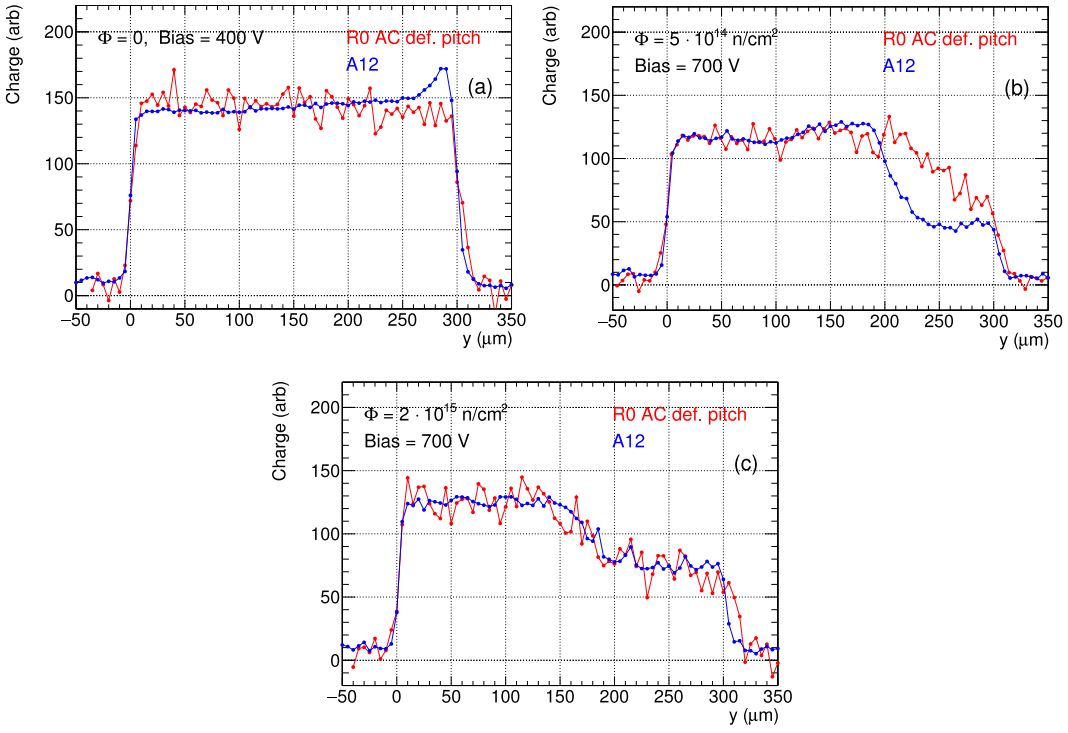

Fig. 11. Charge measured with the edge TCT method in the ATLAS12EC-R0 and A12 sensors for non-irradiated sensors (a), after irradiation with neutrons to 5 10^{14} $n_{eq}cm^{-2}$ (b) and 2 10^{15} $n_{eq}cm^{-2}$ (c).

hundred minutes at 60 °C [21], with a longer time constant than the short-term annealing of the effective dopant concentration [24]. At higher voltages the effect of multiplication [20] can be seen. Short-term annealing initially decreases the effective dopant concentration and consequently the electric field close to the strips, which reduces the multiplication and thus the measured charge. After approximately 1000 min the increase in the effective dopant concentration due to long-term annealing is high enough to stimulate the amplification in high electric fields and the collected charge starts to increase. At the longest annealing time and the highest voltage a charge larger than before the irradiation is measured.

6. Edge TCT measurements

Edge TCT measurements [23] proved to be a very useful tool for the measurement of the electric field in the sensor bulk. Electron hole pairs are generated at a certain depth of the sensor with a narrow (FWHM $\approx$ 8 μm) beam of infrared light (λ = 1060 nm) that penetrates into the detector from the side. The velocity of the charge carriers is probed by the rise of the signal and by scanning the detector with a beam, which allows the velocity as a function of depth in the detector to be measured. Measurements at 200 V for the A12 and R0 sensors with the default pitch are shown in Fig. 10. The difference between the sensors comes from the lower resistivity of the A12 sensors. Therefore, the electric field in R0 expands more deeply than in A12. The measured values for the R0 sensor are more scattered than those of the A12, because the edge of the R0 sensor was not polished; however, this does not affect the conclusions. After irradiation to the highest fluence, this difference diminishes since the concentration of the initial acceptors becomes small compared to the concentration of the acceptors created by the irradiation.

The charge in the edge TCT measurements is defined as the time integral over the signal. If the integration time (in our case 25 ns) is longer than the drift time and there is no trapping like in a non-irradiated detector, the whole charge is measured. In the absence of charge-carrier trapping the measured charge profile (Fig. 11) above the full depletion is uniform along the detector depth. The scales were normalized to give the same average charge in both detectors. These measurements also confirm that the active depths of the A12 and R0 sensors are the same ($\approx$ 300 μm). Before the irradiations the charge profiles in the A12 and ATLAS12-R0 sensors are both uniform, since both sensors are already fully depleted at 400 V and there is no trapping. It is similar for the velocity profile, i.e., the difference in the irradiated sensors diminishes at the highest fluence.

7. Conclusions

We measured the charge collection of the ATLAS12EC-R0 sensors with pitches in the range from 70 to 85 μm and fluences up to 2.2 10^{15} $n_{eq}cm^{-2}$. This range of pitches corresponds to the ATLAS end-cap strip tracker, which will be a part of the future tracker system (ITk). The charge collection is equal for all the pitches at bias voltages below 800 V. This voltage is 100 V higher than the highest voltage foreseen for the ATLAS strip tracker. Above this voltage the multiplication of charge was observed in sensors irradiated with neutrons to the highest fluence. Multiplication is more evident in the sensors with a wider pitch.

Measurement of the charge collection during annealing at 60 °C showed that the multiplication becomes higher at long annealing times when the effective dopant concentration increases.

We did not observe any breakdowns at biases up to 600 V before irradiation and up to 1000 V after irradiation, in accordance with the specifications for the ATLAS ITk sensors. The value of the stable acceptor creation rate for protons (0.004 cm^{-1}) is in agreement with the measurements of previous batches produced for ATLAS by Hamamatsu.

Acknowledgments

The research was supported and financed in part by the Canada Foundation for Innovation, the National Science and Engineering Research Council (NSERC) of Canada under the Research and Technology Instrumentation (RTI) grant SAPEQ-2016-00015; the UK's Science and Technology Facilities Council; USA Department of Energy, Grant DE-SC0010107; European Union's Horizon 2020 Research and Innovation programme under Grant Agreement no. 654168; Slovenian Research Agency (research core funding No. P1-0135 and project ID PR-06802); Ministry of Education, Youth and Sports of the Czech Republic coming from the project LM2015058 - Research infrastructure for experiments at CERN. The authors would like to thank Dr. M. Ito and the accelerator operation staff of CYRIC at Tohoku University for the proton irradiation, and the TRIGA reactor operation staff at Jožef Stefan Institute (JSI) for the neutron irradiation.

References

[1] ATLAS Collaboration, The ATLAS experiment at the CERN large hadron collider, J. Instrum. 3 (8) (2008).
[2] ATLAS-TDR-025. CERN-LHCC-2017.-005. https://cds.cern.ch/record/2257755.
[3] G. Casse, et al., Comparison of charge collection efficiency of segmented silicon detectors made with FZ and MCz p-type silicon substrates, Nucl. Instrum. Methods Phys. Res. A 591 (2008) 178–180.
[4] K. Hara, et al., Charge collection and field profile studies of heavily irradiated strip sensors for the atlas inner tracker upgrade, Nucl. Instrum. Methods Phys. Res. A 831 (2016) 181–188.
[5] R. Mori, et al., Evaluation of the performance of irradiated silicon strip sensors for the forward detector of the atlas inner tracker upgrade, Nucl. Instrum. Methods Phys. Res. A 831 (2016) 207–212.
[6] R. Hunter, et al., First bulk and surface results for the ATLAS ITk Strip stereo annulus sensors - these proceedings.
[7] C. Lacasta, et al., Design of the first full size ATLAS ITk Strip sensor for the endcap region – these proceedings.
[8] G. Lindstroem, et al., Radiation hardness of silicon detectors: a challenge from high-energy physics, Nucl. Instrum. Methods Phys. Res. A 426 (1999) 1–15.
[9] K. Ambrožič, et al., Computational analysis of the dose rates at jsi triga reactor irradiation facilities, Appl. Radiat. Isot. 130 (2017) 1140–1152.
[10] M. Moll, et al., Leakage current of hadron irradiated silicon detectors - material dependence, Nucl. Instrum. Methods Phys. Res. A 426 (1999) 87–93.
[11] D. Žontar, et al., Time development and fux dependence of neutron-irradiation induced defects in silicon pad detector, Nucl. Instrum. Methods Phys. Res. A 426 (1999) 51–55.
[12] A. Chilingarov, Temperature dependence of the current generated in si bulk, J. Instrum. 8 (2013) P10003.
[13] M. Mikestikova, et al., Study of surface properties of atlas12 strip sensors and their radiation resistance, Nucl. Instrum. Methods Phys. Res. A 831 (2016) 197–206.
[14] D. Campbell, et al., Frequency and temperature dependence of the depletion voltage from cv measurements for irradiated si detectors, Nucl. Instrum. Methods Phys. Res. A 492 (2002) 402-210.
[15] G. Kramberger et. al, Modeling of electric field in silicon micro-strip detectors irradiated with neutrons and pions, J. Instrum. 9 (2014) P10016.
[16] R. Marco-Hernandez, et al., IEEE Trans. Nucl. Sci. 56 (2009) 1642–1649.
[17] M. Agari, et al., ALIBAVA: a portable readout system for silicon microstrip sensors, Nucl. Instrum. Methods Phys. Res. A 518 (2004) 468–469.
[18] G. Lindstroem, et al., Radiation hard silicon detectors developments by the RD48 (ROSE) Collaboration, Nucl. Instrum. Methods Phys. Res. A (2001) 308–326.
[19] G. Kramberger, et al., Annealing studies of effective trapping times in silicon detectors, Nucl. Instrum. Methods Phys. Res. A 571 (2007) 608–611.
[20] M. Mikuž, et al., Study of anomalous charge collection efficiency in heavily irradiated silicon strip detectors, Nucl. Instrum. Methods Phys. Res. A 636 (2011) 550–555.
[21] V. Cindro, et al., Radiation damage in p-type silicon irradiated with neutrons and protons, Nucl. Instrum. Methods Phys. Res. A 599 (2009) 60–65.
[22] G. Kramberger, et al., Performance of silicon pad detectors after mixed irradiations with neutrons and fast charged hadrons, Nucl. Instrum. Methods Phys. Res. A 609 (2009) 142–148.
[23] G. Kramberger, et al., Investigation of irradiated silicon detectors by edge-TCT, IEEE Trans. Nucl. Sci. 57 (2010) 2294–2302.
[24] E. Fretwurst, et al., Radiation hardness of silicon detectors for applications in high-energy physics experiments, J. Optoelectron. Adv. Mater. 2 (5) (2000) 575–588.